Progress Report

(2017-2020)

Studies on photocatalytic, photoluminescence and mechanical properties of WS$_2$/C-dot nanoscale systems subjected to irradiation

(UFR-62312)

Submitted by

Principal Investigator

Dr. Dambarudhar Mohanta

Email: best@tezu.ernet.in

Dept. of Physics, Tezpur University

PO:Napaam; Tezpur

Assam-784028

1. Introduction

In recent decades, the 2D materials have drawn growing interest owing to their unique properties and wide range of applications [1,2]. Beyond graphene, 2D materials, like transition metal dichalcogenides (TMDCs), carbon nitride, graphitic carbon (g-C_3N_4), boron nitride (h-B_3N_4) etc. have drawn numerous interest because of their finite and tunable band gaps, low frequency phonon modes and tendency to exfoliate and form mono to few layer systems [3]. Being an important member of the TMDCs family, the WS_2 can grow in layered fashion. Unlike graphene, each layer of the WS_2 is a three atom layer thick structure having thickness of the order of 6-7Å. In-plane atoms are covalently bonded while the weak, van der Waal forces are responsible for binding two consecutive planes [3]. As the van der Waal force is very weak, a small perturbation is sufficient enough to break it and cause exfoliation. This property makes TMDCs in general and WS_2, in particular, a good candidate for the solid lubricants. Structurally, WS_2 may grow in three different structures viz. hexagonal, trigonal and rhombohedral [3,4]. The band gap of bulk WS_2 is typically, ~1.2 eV and that of monolayer is around 2.1 eV. Besides that, the nature of band gap gradually changes from indirect to direct band gap type with exfoliation. Furthermore, the intensity ratio of in-plane (E) to out-of-plane (A) modes is largely dependent on the number of layers as predicted in earlier works [5-7].

In few-layered system, the TMDCs show better luminescence properties. The quantum yield of the system increases rapidly with reduction of the number of layers. As the band-edge emission of the WS_2 lies in the visible region having very fast decay time (few hundreds of ps), so, it is advantageous in technologically important optical and optoelectronic devices. On the other hand, the carbon dot (C-dot) system is well known for its bright emission response and consequently, the WS_2/C-dot system was believed to enhance the optical property of the system at large [8]. Both luminescence and photocatalytic properties are believed to get improved simultaneously in these systems, despite the fact that their origin is quite different from each other.

The year-wise summary of the progress is as detailed below.

2. Summary of first financial year (2017-18)

The approval/sanction letter of the aforesaid project was received in November 2017. After following the general procedure, the project fellow was selected as per Inter University Accelerator Centre (IUAC), New Delhi and Tezpur University rules/regulations. The fellow (Mr. Hemanga Jyoti Sarmah) joined in the department on 18th December 2017. In the first financial year, besides extensive literature survey, material synthesis was carried out following different routes.

As a part of preliminary investigation, layered material specimens were extracted from the exfoliation of the bulk. Subsequently, different exfoliation techniques were adopted and characterized accordingly.

3. Summary of session 2018-19

We have introduced an alternative method of exfoliation, where a superactive polar biomolecule (*collagenase*) was employed as a means of active reagent. In addition, photo-catalytic degradation of harmful dyes was also studied.

Progressive exfoliation of WS₂ system

Here, commercially available bulk tungsten disulfide (WS_2) powder (~2 μm, 99%, Sigma Aldrich) and *Collagenase* (Product No-J62406, 112 kD, Alfa Aesar) were purchased from standard sources. The AR grade acetic acid and sodium hydroxide (NaOH) were obtained from Merck Ltd. and used without further purification. The lyophilized *collagenase* was allowed to disperse in acetic acid at 0.5% (w/v) and then, subjected to magnetic stirring for nearly 1 h, at room temperature. Labeled as G0 specimen, the powder WS_2 was added in 1:1 ratio, followed by stirring and then, subjected to ultrasonication for a

time duration of nearly, 30 min. Subsequently, the sol was neutralized (pH=7) by adding 0.001 M aqueous NaOH. Finally, high speed centrifugation (~8000 rpm) was cogitated for about 10 min. The supernatants were extracted, carefully oven dried and then employed for diffraction, microscopic and spectroscopic characterizations. Depending on the employed treatment time span (2–8 days), the specimens derived were marked as, G2 (2 days), G4 (4 days), G6 (6 days), and G8 (8 days), with G0 (untreated) as reference specimen.
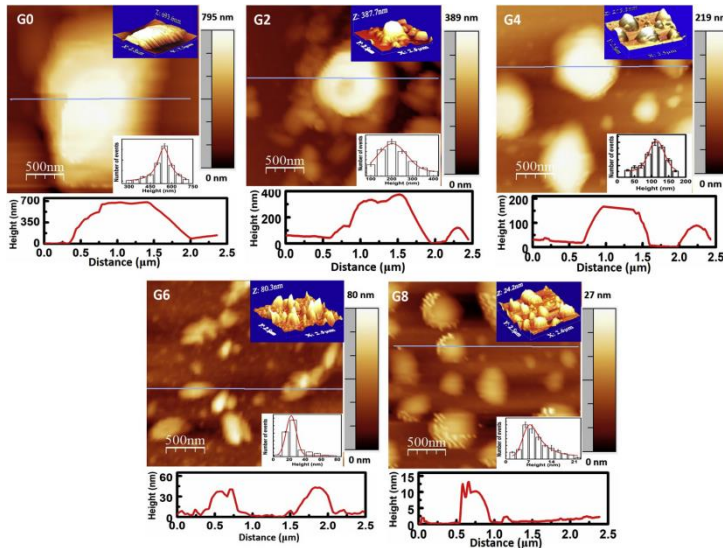

Fig. 1: AFM images of untreated and *collagenase*–treated WS_2 for different duration of treatment (0-8 days). Note, the reduction of height of the sheets with an increasing time duration of treatment with the *collagenase* bio-molecules. In the right upper insets, the 3D topological images of the respective images are shown. Note the conversion of microscopic globular type hillocks to nanoscale rough structures as a result of progressive exfoliation. In the lower panel of each sub-figure, the height profiles corresponded with the selective scan of the WS_2 nanosheets are highlighted.

AFM analysis

As can be found from Fig. 1, the AFM images offer a clear testimony to the layered structures. To assist in the visualization of finer details and in order to acquire a better insight, the 3D topological images are provided in the upper-insets of the respective figures. The height of layers was calculated using multiple scanning steps over the specimen surfaces. The typical height profiles of the selective scans have been depicted at the bottom of the each micrograph. One can now clearly see a bump arising in the height profile of the G0 sample, possibly due to the presence of a micron size stack, while G2, G4 etc. specimens featuring number of bumps with a separation depending on the spacing between the individual stacks. Interestingly, the nature of the height profiles differs from specimen to specimen that would obey Gaussian distribution, and as depicted in the lower-insets of the respective figures. Exfoliation, in terms of number of layers is merely inhomogeneous. Notably, the average thickness drops from as high as, 545±4.8 nm for the untreated WS_2 (G0) to as low as, 7.4±0.7 nm (G8) while the latter describing nearly 10 equivalent layers. Besides the thickness of the sheets, the lateral size of the 2D materials would play crucial role in the design consideration. In our case, the lateral size of G0−G4 specimens is measured to be several micrometers, but it reduces to sub-micron dimensions for G6 and G8 cases. This reduction of size may be because of breaking of strong covalent bonds, as a consequence of longer time of interaction with superactive *Collagenase* molecules. Few layered WS_2 nanosheets having submicron lateral size, is quite suitable for applications in the field of electrode material, catalyst for hydrogen evolution from water, sensor, optoelectronic device fabrication etc [9,10].The nature of decrement of the number of layers with treatment time, *t* is close to the trend of exponential curve fitting, $\sim e^{-0.56t}$ with its pre-exponential factor depending on the initial conditions set prior to exfoliation.
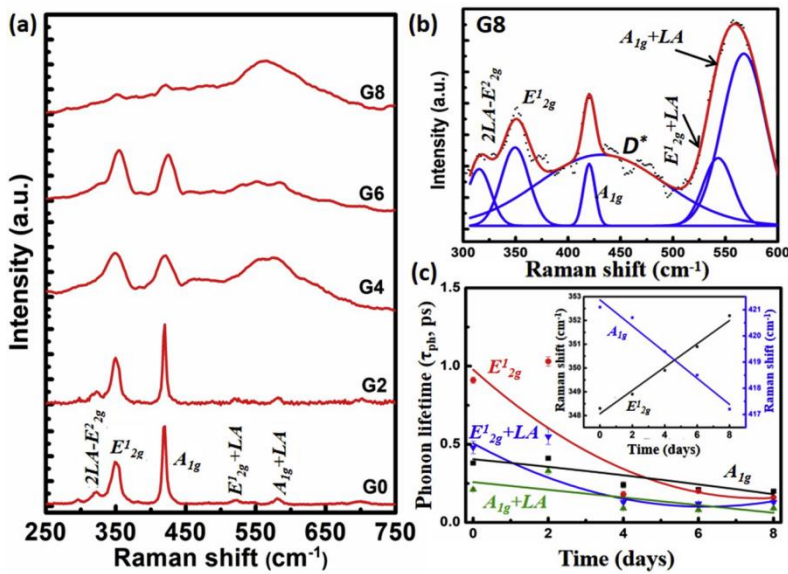
Fig. 2:(a) Raman spectra of *collagenase* treated WS$_2$ with varying interaction time, Note: the Raman active peaks broaden up gradually as we go from G0 to G8, along with the appearance of a new band at ~550 cm^{-1}. (b) deconvoluted modes relevant to G8 system and (c) The declining trend of different Raman active mode life times with treatment time. In the inset, the characteristic shifting of E^1_{2g} and A_{1g} modes with exfoliation time is shown.

Raman spectra analysis

The Raman spectra of the un-exfoliated (G0) and progressively exfoliated (G2-G8) nanoscale WS$_2$ are depicted in Fig. 2(a). In the bulk WS$_2$ system, Raman peaks are located at 324 cm^{-1}, 348.3 cm^{-1}, 421.1 cm^{-1}, 518 cm^{-1} and 581 cm^{-1} which corresponded to the Raman active vibronic modes due to ($2LA$-E^2_{2g}), E^1_{2g}, A_{1g}, (E^1_{2g}+LA) and (A_{1g}+LA); respectively [5].The Raman mode E^1_{2g} corresponds adequate in-plane vibration, while A_{1g} is assigned to the out-of-plane vibration of the successive WS$_2$ layers [6]. Upon treatment of *Collagenase* biomolecules, we observe a three-fold improvement of the E^1_{2g}-to-A_{1g} peak ratio from 0.55 (G0) to 1.5 (G6), signifying effective exfoliation and is in consistency with the earlier works [5].

The evolution of new Raman active band at ~550 cm^{-1} is a consequence of two modes (E^1_{2g}+LA) and (A_{1g}+LA); which tend to improve and get broadened eventually with prolonged *collagenase* interaction. The Raman active modes for the G8 case, can be found in the deconvoluted spectra shown in Fig. 2(b). Here, we can see ($2LA$-E^2_{2g}), E^1_{2g}, A_{1g}, (E^1_{2g}+LA) and (A_{1g}+LA) modes after deconvolution. As can be seen from Fig. 2(b), in G8 case, a broad peak (D*) located at ~430 cm^{-1}, appears due to possible sulphur vacancies in consistent with the existing literature [11]. In G6 and G8 cases, the appearance of this new band ~550 cm^{-1} or the improvement of (E^1_{2g}+LA) and (A_{1g}+LA) may be attributed to flavouring longitudinal acoustic mode (LA) vibrations in few layered structure [12]. A decline trend of phonon lifetime for the Raman active mode can be seen in the Fig. 2(c). Besides that, a prominent shifting of A and E mode can be seen in the inset of the same figure. The details can be found at, https://doi.org/10.1016/j.matchemphys.2020.123008

Photocatalytic degradation of harmful dyes

In order to analyze the photocatalytic degradation efficiency, we opted *malachite green* (MG) and *methyl ora*nge (MO) as the targets and WS$_2$/C-dot hybrid systems as the nanocatalyst. The MG is an organic compound that is used as a dye-stuff and controversially, as an antimicrobial agent in aquaculture.

The UV–Vis optical absorption responses of the organic dyes and the nanocatalyst-loaded MO and MG systems can be found in Fig. 3 and Fig. 4 (col.1). Recognizing untreated MO and MG peak maxima at ~456 nm and 617 nm, as can be noticed, the absorbance shows a steady fall with an increasing exposure time. Whereas, MO characterizes broad spectral characteristics, MG gave a steep spectral

feature. Qualitatively, when exposed to visible light for a time duration of 60 min., we obtained respective photodegradation efficiency of ~72.3% and 83.2% for the MO and MG dyes with the inclusion of bare WS_2 nanosheets as the photocatalyst (Fig.3, col.2) [8]. Surprisingly, the degradation efficacy of the MO and MG dyes, in presence of WS_2/C-dot nanocatalyst was estimated to be, ~81.2% and 91%; respectively (Fig.4, col2). Moreover, the photodegradation response was seen to be much rapid in case of MG than the case for MO dye, possibly because of its strong sensitivity to the red part of the visible light (Fig.4, col.2) [8].
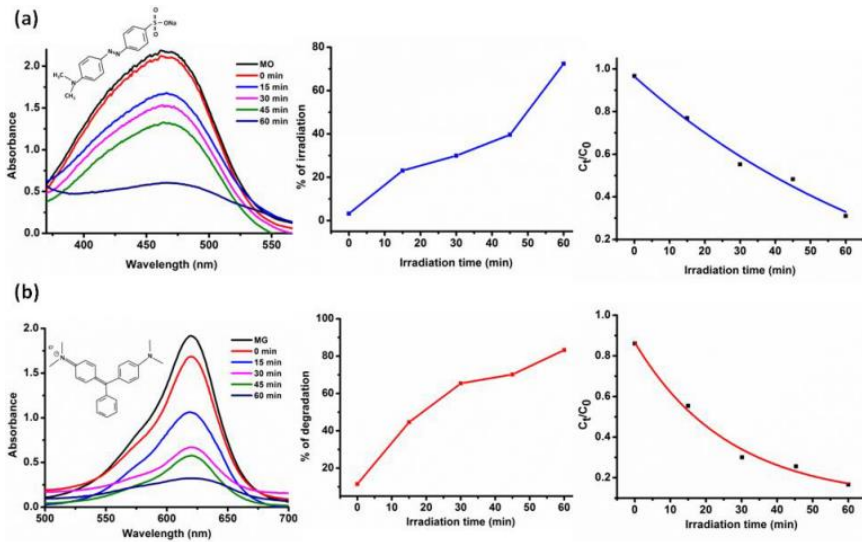

Fig. 3: Optical absorption spectral features illustrating photodegradation of (a) MO, and (b) MG dyes under visible light illumination and using WS_2 nanosheets as the desired nanocatalyst. The exact nature of degradation with exposure time can be found in col.2 and col.3.
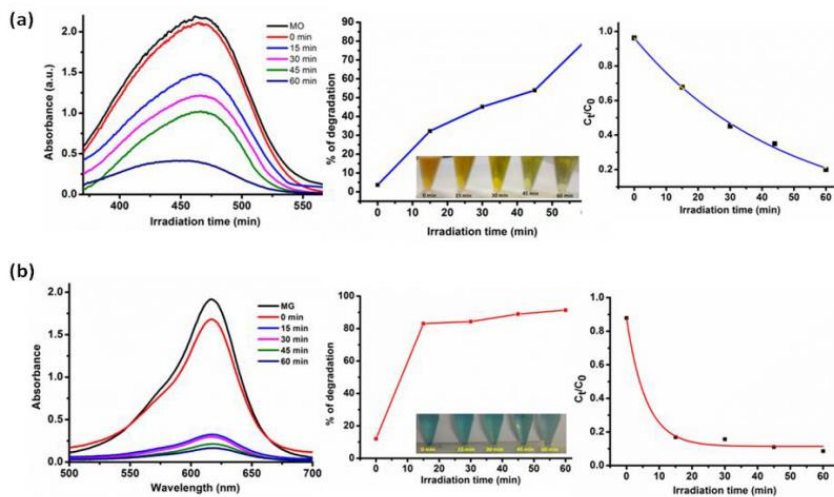

Fig. 4: Optical absorption spectral features illustrating photodegradation of (a) MO, and (b) MG dyes under visible light illumination and using WS_2/C-dot nanosheets as the desired nanocatalyst. The exact nature of degradation with exposure time can be found in col.2 and col.3.

Here, we employ the Langmuir– Hinshelwood (L-H) kinetics model to assess rate constants [15]. The rate constants (k_a), as directly obtained from the nature of the curves and using the model equation, are estimated to be, 0.012 min^{-1} and 0.058 min^{-1} when MO and MG dyes were loaded with the WS$_2$ nanosheets; respectively. In contrast, WS$_2$/C-dot loaded MO and MG systems gave respective k_a values as, 0.0215 min^{-1} and 0.168 min^{-1}. Apparently, the WS$_2$/C-dot nanohybrid is extremely sensitive to the photoactivity as compared to its bare nanosheet counterpart [8].

4. Session 2019-20

In the second year, we have investigated the optoelectronic properties of few layered WS$_2$ systems, subjected to energetic γ and β irradiation effects. Our earlier plan of irradiating specimens with swift heavy ions could not be realized in the absence of a proper time slot. However, steady state photoluminescence (PL) and time resolved photo-luminescence (TR-PL) studies were performed on our layered systems considering γ and β irradiation effects.
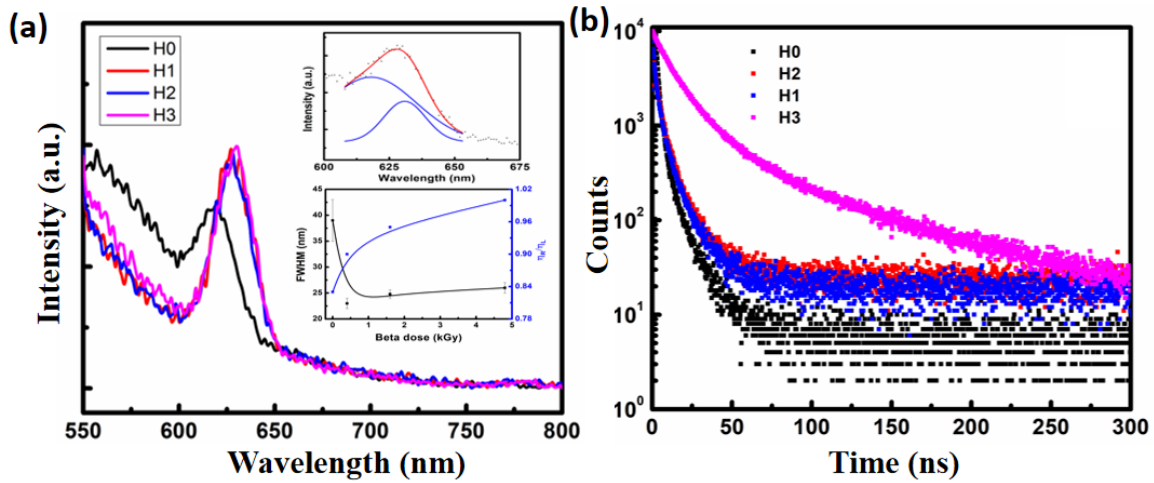

Fig. 5: The luminescence spectra of pristine and irradiated WS$_2$ systems. In the upper inset, the deconvoluted spectra of the pristine sample can be seen, whereas, the variation of the FWHM and the η_R/η_L can be noticed in the lower inset. Note: Upon deconvolution, we notice two distinct peaks corresponding to the band edge emission and trionic emission; respectively. Time resolved photo-luminescence spectra of the specimens are depicted in the Fig. (b).

Impact of energetic β-particles on WS$_2$ systems

Circular pellets (dia ~1 cm) of WS$_2$ were made with the help of a hydraulic press by applying a normal pressure of 60 kbar, for 5 min. The prepared pellets of WS$_2$ were put in a closed β-radiation chamber available in the PG laboratory of our department (^{137}Cs source, activity=0.4 kGy/hour). The samples were irradiated in ambient environment (300 K), but with varying doses 0 kGy, 0.4 kGy, 1.6 kGy and 4.8 kGy. The WS$_2$ samples are labelled as, *H0*, *H1*, *H2* and *H3* which correspond to a β-dose of 0 kGy, 0.4 kGy, 1.6 kGy and 4.8 kGy.

Influence on the luminescence response

The emission spectra of the WS$_2$ systems are shown in Fig. 5(a). As can be visualized, the emission peak at ~624 nm corresponds the band gap emission of the system (λ_{ex}~525 nm) [13]. A clear enhancement of the FWHM of the emission peak, from 22 nm to 39 nm has been witnessed for WS$_2$. Upon irradiation, this emission peak shows a red shift from ~624 nm (*H0*) to 630 nm (*H3*). This shifting may be encountered for probable conversion of neutral excitons to trions. TR-PL is a standard method to study

the life time decay dynamics of the radiative emission peak/profile for which a pico-second pulsed laser was employed to excite the system. The decay responses corresponding to the emission peak, can be found in Fig. 5(b). In all the cases, we observe a bi-exponential feature of the decay response fitted to the formula: $A = A_1 e^{-t/\tau_1} + A_2 e^{-t/\tau_2}$; where, τ_1 and τ_2 are fast and slow parameters corresponding to the radiative band-to-band transition and non-radiative transitions by virtue of transition from the conduction band to the trap states, followed by radiative emission from the intermediate states to the valence band; respectively. A slow-down of the slow parameter is witnessed as a consequence of the irradiation induced defects in the system. The slow parameter (τ_2) tending to be slower, from 2.23±0.04 ns (H0) to 15.84±0.04 ns (H3). At the same time, the fast parameter (τ_1), i.e., 0.39 ns remains almost unaltered during the irradiation process (up to 3% variation). The average lifetime of the decay can be estimated using the formula [14]: $\tau_{av} = \frac{\tau_1 \tau_2}{\tau_1 + \tau_2}$. Here, we found an improvement of the average lifetime of the system with the increasing of β-doses. A rapid recombination in the defect sites may be responsible for the enhancement of the average decay parameter with β- irradiation effect. We also observe an enhancement in the quantum yield of the WS_2 system, from a value of ~84% to 95% upon irradiation effect.

Impact of energetic γ-irradiation on WS_2 systems

The WS_2 systems were exfoliated via a solvo-sonication method, and were put in a shield chamber for γ-irradiation. Co^{137} has been used as a standard source for γ-irradiation (1.75 kGy/h). The selected doses considered were, 12kGy, 34 kGy, 48 kGy and 96 kGy, and labeled as G1, G2, G3 and G4; respectively. The pristine (0 kGy) was kept as reference sample, G0.

Exciton- to- trionic conversion

The steady state PL emission spectra (λ_{ex}= 500 nm) of the pristine and γ-ray irradiated WS_2 nanosheets are shown in Fig. 6(a). The figure essentially depicts a series of asymmetrically broadened spectra with the near band edge emission (NBE) or excitonic peak located at ~605 nm. On varying γ-doses and even up to 96 kGy, we noticed a defect mediated emission (DE) peak located at ~680 nm, with the nature of the band edge maxima remaining unaltered. Owing to the creation of sulphur vacancies and charged defect centers, the DE peak intensity was seen to shoot up invariably with the increasing γ-dose (G1–G4). The absence of the DE peak for the pristine WS_2 system (G0) suggests that the origin of these defects lies in the complete removal or dislodgement of atoms induced by the energetic γ-rays. We also captured the NBE emission response in perpendicular directions (*s*-and *p*-polarizations) and consequently, anisotropy and degree of polarization can be determined, as shown in the inset of Fig. 6(a). While both these parameters follow nearly similar and steady declining trends with the variation in γ-doses, the γ-irradiated WS_2 nanosheets (G4) exhibited an observably suppressed polarization sensitivity by ~72%. The emission peak at ~630 nm corresponds to charged excitonic emission (trion), which seems to improve till a critical dose has been achieved. This could be because of conversion of adequate neutral excitons to charged excitons, as a consequence of γ-irradiation. It is worth noting here that, trions are quite unstable and represent an intermediate class of quasi-particles which lie in between stable conformations of excitons and bi-excitons. For instance, interactions among the individual excitons (*e,h*) result in the bound states, called biexcitons (*e, h; e, h*). Any combination of (*e; e,h*) or (*e, h; h*) can never be neutral, and can form virtual bound states, i.e., trions, which are nothing but charged excitons at large. In order to exploit this further in terms of the partial conversion of neutral excitons to trions, and how defects manifest in reference to the excitons, we plotted different (normalized) PL emission intensity ratios, depicted in Fig. 6(b). Presuming that the concentration of excitons remaining constant, a slow rising trend of I_{630}/I_{605} with increasing dose indicates adequate conversion of neutral excitons to charged ones via the capturing of either a free electron or a hole. The manifestation of excitons into trions has
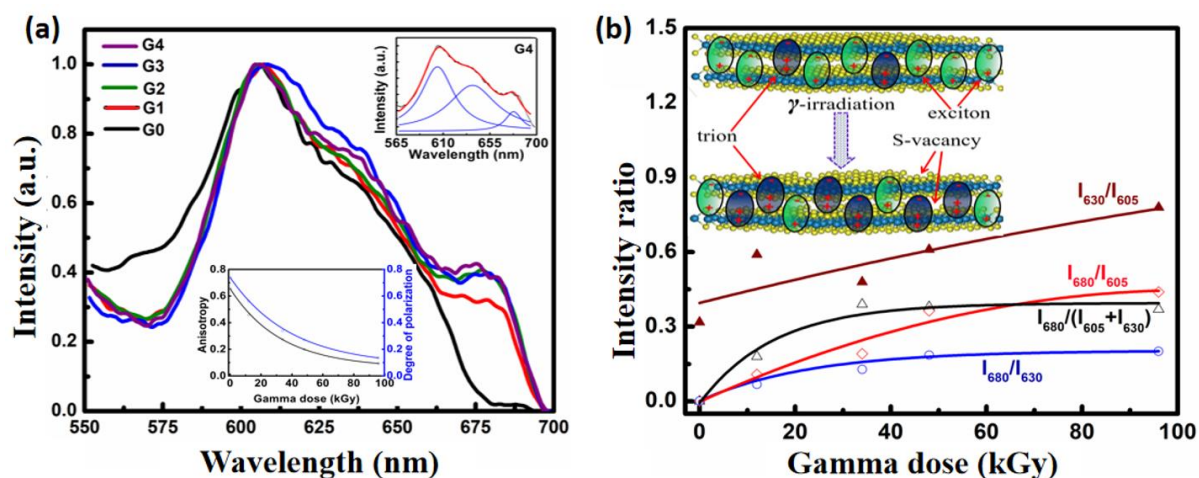
Fig. 6:(a) Photo-luminescence spectra of pristine and gamma irradiated nanoscale WS_2 systems. A de-convoluted spectra for G4 and variation of anisotropy and polarization can be seen in the inset. (b) Relative variation of different luminescence peaks along with a scheme (inset) that depicts possible exciton-to-trion conversion phenomenon.

been illustrated schematically as inset of Fig. 6(b). Nevertheless, the evolution of the DE peak was such that, while I_{680}/I_{605} and I_{680}/I_{630} gave exponentially growing trends, $I_{680}/(I_{630}+ I_{605})$ predicts an asymptotic behaviour. Interestingly, the rate of growth of defect mediated emission with reference to neutral excitons was noticeably higher than the charged excitons, though it remains unclear as to whether defects actually help in the conversion process or relics as stand-alone phenomena. (Besides these, we also observed 1T phase formation, improvement of spin densities and defect mediated vibration modes, which can be tracked in the link, https://doi.org/10.1088/1361-6528/ab7c4a.

As for mechanical studies, only inorganic fullerene (IF-type) WS_2/PVA systems have been worked out with the help of a universal testing machine (UTM; Zwick, BZ010/TN2S) to examine the tensile strength and toughness. Mechanical properties, as evaluated through the stress vs. strain measurements, generally improve with increasing loading, however, it drops at 10wt% nano-IF WS_2 due to the overcrowding effect. In contrast, the tribological behavior was assessed by a TwinedriveTM Rheometer (AntonPaar, MCR 702, Graz, Austria). The coefficient of viscosity at maximum velocity is drastically lowered when an increased loading was considered. The detailed discussion is available at https://link.springer.com/article/10.1557%2Fjmr.2019.301

Thanks to the AnotonPaar's Analytical division at Gurgaon.

The WS_2 nanosheet samples could not be worked out due to a lack of available time slot and feasibility which could have helped us making a comparative study on rheological aspects using different morphologies of the material.

5. Session 2020-21

The data acquired were properly analyzed as per requirement. Although some studies could not be executed as per the earlier plan, many objectives could be fulfilled through this project. Our results also indicated new opportunities/challenges which can be explored further. The final UC/SE and comprehensive reports are prepared at the end.

References

[1] J. N. Coleman et. al., Science **331**(6017), 568 (2011).

[2] R. Mas-Balleste, C. Gomez-Navarro, J. Gomez-Herrero, and F. Zamora, Nanoscale **3**(1), 20 (2011).

[3] S. Manzeli, D. Ovchinnikov, D. Pasquier, O. V. Yazyev, and A. Kis, Nat. Rev. Mater. **2**(8), 17033, (2017).

[4] Q. H. Wang, K. Kalantar-Zadeh, A. Kis, J. N. Coleman, and M. S. Strano. Nat. Nanotech. **7**(11), 699 (2012).

[5] A. Berkdemir et. al., Sci. Rep. **3**, 1755 (2013).

[6] M. Thripuranthaka, R.V. Kashid, R. C Sekhar and D.J. Late, Appl. Phys. Lett.**104**(8), 081911 (2014).

[7] A. Molina-Sanchez and L. Wirtz, Phys. Rev. B**84**, 155413 (2011).

[8] S. J. Hazarika and D. Mohanta, J. Lumin., **206**, 530 (2019).

[9] S.K.Balasingam, J.S.Lee, Y. Jun, Dalton Transactions, **44**(35), 15491-15498 (2015).

[10] N.Perea López et. al., Adv. Funct. Mater., **23**(44), 5511-5517 (2013).

[11] C.Lee, B.G.Jeong, S.J.Yun,Y.H. Lee, S.M. Lee and M.S.Jeong, ACS Nano, **12**(10), 9982-9990 (2018).

[12] A.P.Gaur, S.Sahoo, J.F. Scott and R.S.Katiyar, J. Phys. Chem. C, **119**(9), 5146-5151 (2015).

[13] B. J Modtland, E. Navarro-Moratalla, X. Ji, M. Baldo, and J. Kong, Small, 13(33), 1701232 (2017).

[14] L.Yuan and L. Huang, Nanoscale,**7**(16), 7402-7408 (2015).

[15] U.I. Gaya, A.H. Abdullah, J. Photochem. Photobiol. C 9, 1–12 (2008).

Outcome

Journal Publications

1. H.J. Sarmah, A. Deka, P. Kulriya, D. Mohanta, Europhys. Lett., 125(3), 36003 (2019)

2. S.J. Hazarika, D. Mohanta, J. Luminesc. 206, 530 (2019).

3. H.J. Sarmah, D. Mohanta and A. Saha, Nanotechnology, 31, 285706 (2020)

4. H.J. Sarmah and D. Mohanta, Mater. Chem. Phys. 250, 123008 (2020)

5. H.J. Sarmah, A. Saha and D. Mohanta, J. Mat. Res. 36, 870-883 (2021).

6. H.J. Sarmah and D. Mohanta, J. Mat. Res., (2021) (In press). DOI: 10.1557/s43578-021-00211-8

Conference presentations

1. Spontaneous exfoliation of tungsten disulfide and characterizations, Condensed Matter Days (CMDAYS18), 29-31 August 2018, Burdwan University, Burdwan, W.B.

2. Effect of gamma photons on tungsten disulfide nanosystem, Frontiers in Chemical Sciences (FICS), 6-8 December 2018, IIT Guwahati, Guwahati.

3. Theoretical density functional calculation of monolayered WS_2, National seminar on Theoretical and Condensed Matter Physics, 20&21 December 2018, ADP College, Assam,.

4. Effect of irradiation on layered materials, Science and Technology using Ion Beams and Gamma Irradiation Workshop, 28&29 December 2019, VECC, Kolkata.

5. Evidence of exciton-to- trion conversion process in 2D tungsten disulphide (WS_2) sheets subjected to energetic β and γ irradiation, Condensed Matter Days (CMDAYS20), 10-13 December 2020, NIT Silchar.

***

COMPREHENSIVE FUND UTILIZATION CERTIFICATE
(2017-2021)

(Projects/Schemes)

Name of Nodal Institute/Department
of Organization   : **Tezpur University**

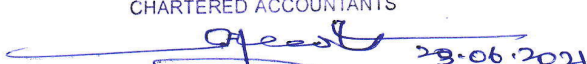Scheme   :   UFR-62312
Funding Agency   : IUAC, New Delhi

Name of Project   : Studies on photocatalytic, photoluminescence and mechanical properties of WS_2/C-dot nanoscale systems subjected to irradiation

Certified that out of **Rs. 8,45,578/-** (Rs. 80,467/- + Rs. 2,17,000/-+ Rs. 3,09,234/- + Rs. 2,38,877/- during 2017-18, 2018-19, 2019-20 and 2020-21; respectively) received from **IUAC, New Delhi** as per sanction letter **IUAC/XIII.7/UFR-62312,** a sum of **Rs. 8,45,066/-** (Rs. 80,467/-+ Rs. 2,17,000/- +Rs. 3,08,244/- + Rs. 2,39,355/- during respective years of 2017-18, 2018-19, 2019-20 and 2020-21) has been utilized for the purpose for which it was sanctioned. The unspent amount of Rs. 512/- being transferred through electronic transfer/cheque number 669416, NEFT UTR No. SBIN521082334042 dtd. 23/Mar/2021 from TU A/C number 30448821505.

Principal Investigator
Principal Investigator
DST-SERB/IUAC/CSIR Project
Department of Physics
Tezpur University

Finance Officer
(Tezpur University)
Finance Officer
Tezpur University

For SURAJIT CHAKRABORTY & CO.
CHARTERED ACCOUNTANTS

28.06.2021

CA. SURAJIT CHAKRABORTY
(Proprietor)
Membership No.- 305054

COMPREHENSIVE EXPENDITURE STATEMENT OF IUAC (UFR-62312) PROJECT (Year 2017-2021)

Title: '*Studies on photocatalytic, photoluminescence and mechanical properties of WS_2/C-dot nanoscale systems subjected to irradiation*'

UFR-62312
Funding Agency: IUAC, New Delhi

Serial Number	Academic year	Heads of account	Received amount (Rs.)	Expenditure (Rs.)	Unspent/committed Balance (Rs.)
1	2017-2018	Fellowship	55,467/-	55,467/-	0/-
		Contingency	25,000/-	25,000/-	0/-
2	2018-2019	Fellowship	1,92,000/-	1,92,000/-	0/-
		Contingency	25,000/-	25,000/-	0/-
3	2019-2020	Fellowship	2,84,234/-	2,83,355/-	879/-
		Contingency	25,000/-	24,889/-	111/-
4	2020-2021	Fellowship	2,38,877/-	2,39,355/-	(-)478/-
		Contingency	----	-----	-----
		Total	8,45,578/-	8,45,066/-	*512/-

*The unspent amount of Rs. 512/- being transferred through electronic transfer/cheque number 669416 NEFT UTR No. SBIN521082334042 dtd. 23/Mar/2021 from TU A/C No. 30448821505.

Registrar

Tezpur University
Registrar
Tezpur University

Finance Officer

Tezpur University
Finance Officer
Tezpur University

For SURAJIT CHAKRABORTY & CO.
CHARTERED ACCOUNTANTS

23·06·2021

CA. SURAJIT CHAKRABORTY
(Proprietor)
Membership No.- 306054